Accepted Manuscript

Boronic ester-linked macrocyclic lipopeptides as serine protease inhibitors targeting *Escherichia coli* type I signal peptidase

Natalia Szałaj, Lu Lu, Andrea Benediktsdottir, Edouard Zamaratski, Sha Cao, Gustav Olanders, Charles Hedgecock, Anders Karlén, Máté Erdélyi, Diarmaid Hughes, Sherry L. Mowbray, Peter Brandt

PII: S0223-5234(18)30758-X

DOI: 10.1016/j.ejmech.2018.08.086

Reference: EJMECH 10697

To appear in: *European Journal of Medicinal Chemistry*

Received Date: 9 July 2018

Revised Date: 22 August 2018

Accepted Date: 29 August 2018

Please cite this article as: N. Szałaj, L. Lu, A. Benediktsdottir, E. Zamaratski, S. Cao, G. Olanders, C. Hedgecock, A. Karlén, Máé. Erdélyi, D. Hughes, S.L. Mowbray, P. Brandt, Boronic ester-linked macrocyclic lipopeptides as serine protease inhibitors targeting *Escherichia coli* type I signal peptidase, *European Journal of Medicinal Chemistry* (2018), doi: 10.1016/j.ejmech.2018.08.086.

Boronic ester-linked macrocyclic lipopeptides as serine protease inhibitors targeting *Escherichia coli* type I signal peptidase.

Natalia Szałaj [a, †], Lu Lu [b, †], Andrea Benediktsdottir [a], Edouard Zamaratski [a], Sha Cao [c], Gustav Olanders [a], Charles Hedgecock [a], Anders Karlén [a], Máté Erdélyi [d], Diarmaid Hughes [c], Sherry L. Mowbray [b, *], Peter Brandt [a, *]

[a] Department of Medicinal Chemistry, Uppsala University, Box 574, SE-751 23 Uppsala, Sweden.

[b] Department of Cell and Molecular Biology, Uppsala University, Box 596, SE-751 24 Uppsala, Sweden.

[c] Department of Medical Biochemistry and Microbiology, Uppsala University, Box 582, SE-75 123 Uppsala, Sweden.

[d] Department of Chemistry – BMC, Uppsala University, SE-751 23 Uppsala, Sweden.

[†] N.S. and L.L. have contributed equally to this work and should both be considered as first authors.

* Corresponding authors. Tel.: +46 18 471 49 90. E-mail address: sherry.mowbray@icm.uu.se (S. L. Mowbray). Tel.: +46 18 471 43 94. E-mail address: peter.brandt@ilk.uu.se (P. Brandt).

ABSTRACT

Type I signal peptidase, with its vital role in bacterial viability, is a promising but underexploited antibacterial drug target. In the light of steadily increasing rates of antimicrobial resistance, we have developed novel macrocyclic lipopeptides, linking P2 and P1' by a boronic ester warhead, capable of inhibiting *Escherichia coli* type I signal peptidase (*Ec*LepB) and exhibiting good antibacterial activity. Structural modifications of the macrocyclic ring, the peptide sequence and the lipophilic tail led us to 14 novel macrocyclic boronic esters. It could be shown that macrocyclization is well tolerated in terms of *Ec*LepB inhibition and antibacterial activity. Among the synthesized macrocycles, potent enzyme inhibitors in the low nanomolar range (e.g. compound **42f**, *Ec*LepB IC_{50} = 29 nM) were identified also showing good antimicrobial activity (e.g. compound **42b**, *E. coli* WT MIC = 16 µg/mL). The unique macrocyclic boronic esters described here were based on previously published linear lipopeptidic *Ec*LepB inhibitors in an attempt to address cytotoxicity and

hemolysis. We show herein that structural changes to the macrocyclic ring influence both the cytotoxicity and hemolytic activity suggesting that the P2 to P1' linker provide means for optimizing off-target effects. However, for the present set of compounds we were not able to separate the antibacterial activity and cytotoxic effect.

GRAPHICAL ABSTRACT

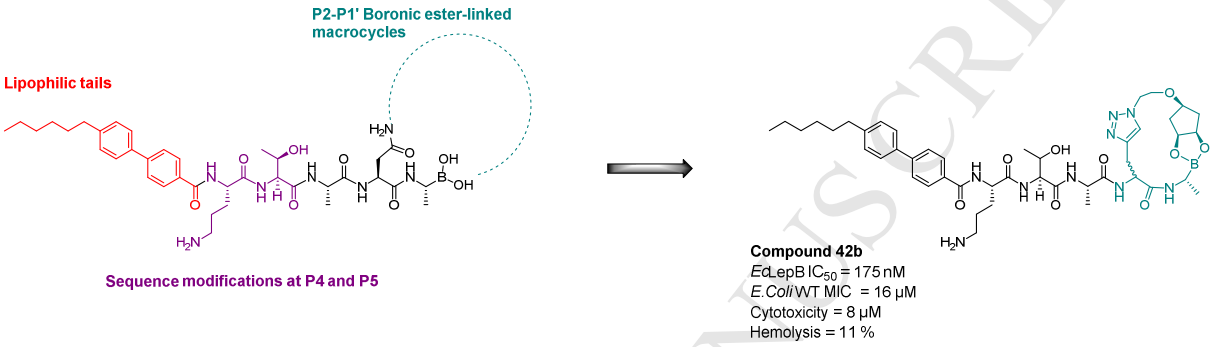

Keywords

P2–P1' Boronic ester-linked macrocycles

Antibacterial lipopeptides

Bacterial type I signal peptidase

Escherichia coli type I signal peptidase (*Ec*LepB)

Highlights

- First-in-class P2–P1' boronic ester-linked macrocyclic lipopeptides.
- Compounds are potent inhibitors of bacterial type I signal peptidase (LepB).
- Good antibacterial activity was shown for macrocycles.
- The antibacterial effect and cytotoxicity could not be separated.
- The macrocyclic boronic esters can be used for inhibition of serine proteases.

Abbreviations

2-CTC 2-chlorotritylchloride

AMR antimicrobial resistance

CuAAC copper(I)-catalyzed azide-alkyne cycloaddition

DCM dichloromethane

DIEA *N, N*-diisopropylethylamine

DMF dimethylformamide

DMSO dimethyl sulfoxide

E. coli *Escherichia coli*

***Ec*LepB** *Escherichia coli* type I signal peptidase

FMCA fluorometric microculture cytotoxicity assay

Fmoc 9-fluorenylmethyloxycarbonyl

HBTU *N, N, N′,N′*-tetramethyl-*O*-(1*H*-benzotriazol-1-yl)uronium hexafluorophosphate

HFIP 1,1,1,3,3,3-hexafluoro-2-propanol

LiOH lithium hydroxide

MeOH methanol

NMO 4-methylmorpholine *N*-oxide

TBAF tetra-*n*-butylammonium fluoride

SPase I bacterial type I signal peptidase

TFA trifluoroacetic acid

1. Introduction

The high frequency of antimicrobial resistance (AMR) presents a global health emergency according to a recent report by the World Health Organization [1]. Largely due to widespread antibiotic misuse, resistance has made formerly treatable diseases deadly again [2]. Currently, the number of deaths from bacterial infections is estimated at 2 million people a year, and projected to quintuple by 2050 [3]. These facts show that antimicrobial resistance places a considerable burden on society and healthcare systems, and highlight the importance of developing new antibiotics to replace those that are no longer useful. The current WHO

priority pathogens list has a strong focus on Gram-negative bacteria, including *Escherichia coli* (*E. coli*), in its highest-priority ("critical") category for which new antibiotics are needed [4].

Bacterial type I signal peptidase (EC 3.4.21.89, SPase I), a membrane-bound serine endopeptidase, recognizes and cleaves the N-terminal signal peptide found in the majority of pre-proteins that are translocated across membranes *via* the Sec and Tat pathways. This allows the secretion of a large number of mature proteins that are critical for the survival and virulence of bacteria [5,6]. In contrast to classical Ser/His/Asp proteases, and to type I signal peptidases from the eukaryotic endoplasmic reticulum that act through a Ser/His dyad, bacterial type I signal peptidases act through a unique Ser/Lys catalytic dyad, which is conserved in both Gram-positive and Gram-negative species [7]. Their role in bacterial viability, together with the afore mentioned differences in the mode of action and the relatively accessible position of its active site on the outer surface of the cytoplasmic membrane, make this enzyme a promising but underexploited antibacterial drug target [8]. Only a few distinct groups of signal peptidase inhibitors have been reported, including the macrocyclic arylomycin family (lipopeptides) [9–11], krisynomycin [12], 5*S*-penems (β-lactams) [13–16], oligopeptides [17,18] and a beta-aminoketone [19,20]. Many opportunities thus remain for antibacterial drug discovery.

To be effective, new classes of antibiotics must overcome the general problems of entry into the cell, susceptibility to active efflux, and possible toxicity caused by the lack of selectivity between bacterial and mammalian cells [21]. Periplasmic enzymes, such as SPase I, have advantages when developing antibiotics that target Gram-negative bacteria, as such drugs need only to pass the outer membrane of the double-membrane structure. Macrocycles, which have been predominantly developed for treatment of infectious disease and for use in oncology [22], have several features that can help overcome the problems listed above. Due to their structural preorganization combined with some residual remaining flexibility, macrocycles can interact both with shallow binding sites and dynamic protein targets. In addition macrocyclization also has the potential to increase both binding affinity and selectivity [23]. It has been shown that macrocyclization can be designed for improved membrane permeability [24–26], metabolic stability [27,28] and pharmacokinetics [29]. In addition, the number of cyclic peptide natural products with demonstrated oral bioavailability suggests that mid-sized peptidic macrocycles may display favorable physicochemical properties beyond the rule of five [30]. Thus, medicinal chemists have become increasingly interested in macrocyclic compounds for expanding druggable space.

In our own work, we decided to develop macrocyclic oligopeptides, aiming at inhibition of the *E. coli* SPase I (*Ec*LepB) and having antibacterial activity. Here we report the design, synthesis and biological evaluation of first-in-class P2–P1' boronic ester-linked macrocyclic lipopeptides. We assessed their inhibition of *Ec*LepB, as well as antibacterial activity against a panel of Gram-negative strains. Further, tests of cytotoxicity and hemolysis were carried out as a preliminary investigation of safety.

2. Chemistry

2.1 Design

Recently, our group reported on linear lipopeptides [31] based on the decanoyl-PTANA-aldehyde *Ec*LepB inhibitor published by Buzder-Lantos *et al.* [18]. We showed that replacing the aldehyde by a boronic ester improved the *Ec*LepB IC_{50} 50-fold, and that boronic esters and acids were equipotent. However, modest antibacterial activity combined with cytotoxicity limited their potential as leads for drugs. Since extensive optimizations of similar lipopeptide *Ec*LepB inhibitors, including arylomycin-like macrocycles, have been published in recent patent literature [32,33], there was an interest to explore novel chemical space to address the toxicity issues. Therefore, we searched for alternative sites for macrocyclization allowing for chemistry different from previous inhibitors. As arylomycin is cyclized between P2 and P4 and the side-chains of P1 and P3 are buried in hydrophobic pockets in the enzyme, we focused on a novel alternative cyclization between P2 and P1' (see Figure 1). The P1' position corresponds to the diol attached to the boron in the warhead. Macrocyclic boronic esters, usually containing more than one boron atom, have mostly been studied in supramolecular chemistry [34]. To the best of our knowledge, this is the first report of boronic ester-linked macrocycles being used as protease inhibitors.

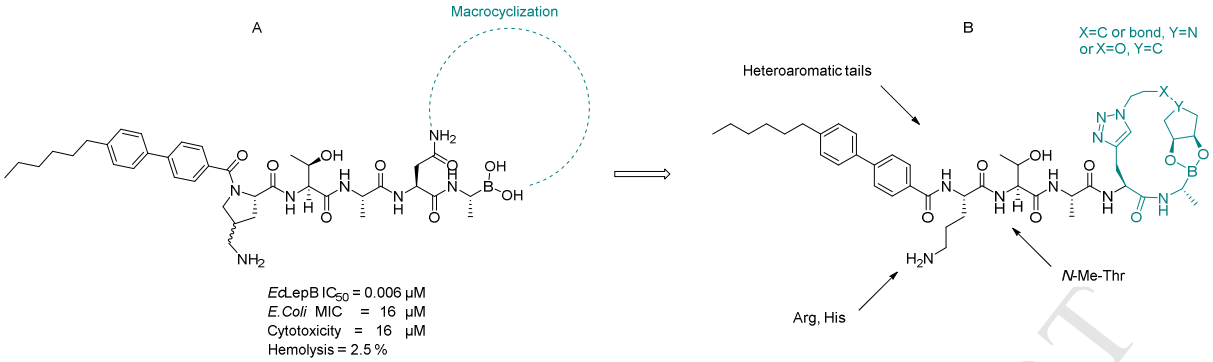

Figure 1. Design of the boronic ester macrocyclic oligopeptides (B) based on previously reported linear *Ec*LepB inhibitor (A).

We started by investigating the conformational preference of the peptidic backbone upon P2–P1' macrocyclization, to rule out the possibility that the cyclization would destabilize the bioactive conformation of the peptide or the boronic ester. The initial calculations were performed using a 3,4-dihydroxypyrrolidine boronic ester linked to a P2 cysteine, aspartic acid or glutamic acid, with amides, thioethers and disulfides as linkers. However, as the original hit had an asparagine in P2, it made sense to keep this in the cyclized analogue. To facilitate the synthesis, the amide was replaced by a triazole, an excellent peptide-bond isostere that can easily be formed by the 'Click' reaction both in solution and on a solid support [35]. Modelling different chain lengths between the P2 substituent and the boron-capturing diol suggested that variants including 2–5 atoms all gave reasonable structures. By means of density functional theory calculations, the macrocyclizations were estimated to be energetically favored; see Supplementary Material for details. The final design featured three unique boronic ester macrocyclic scaffolds; a *cis*-pyrrolidine-3,4-diol boronic ester with either an ethylene or a propylene linker, and an all-*cis* cyclopentane-1,2,4-triol boronic ester with an ethylene linker as shown in Figure 1. We also decided to slightly modify the oligopeptide sequence at positions P4 and P5, and to investigate changes to the lipophilic tails at the N-terminus.

As a positive charge at P5 is crucial for MIC activity in this series [31], we used commercial ornithine instead of the 4-aminomethyl proline to simplify the synthesis without compromising the potency (for examples, see **31g** and **31h** in Table 1).

2.1.1. Structure-based design

The three selected macrocyclic structures, truncated at the N-terminus, were further investigated by means of conformational sampling of the covalent protein-macrocycle complexes. It was concluded that all three macrocycles could fit the *Ec*LepB binding site with backbone conformations identical to arylomycin and a non-cyclized analogue, as shown in

Figure 2. Overlays of arylomycin A2, the linear analogue, and a pyrrolidine-based macrocycle in the predicted protein-bound conformations are shown in Figure 3. The different linker lengths did not disturb the backbone conformation of the macrocyclic compounds compared to the linear analogue (see Figures 2 and 3).

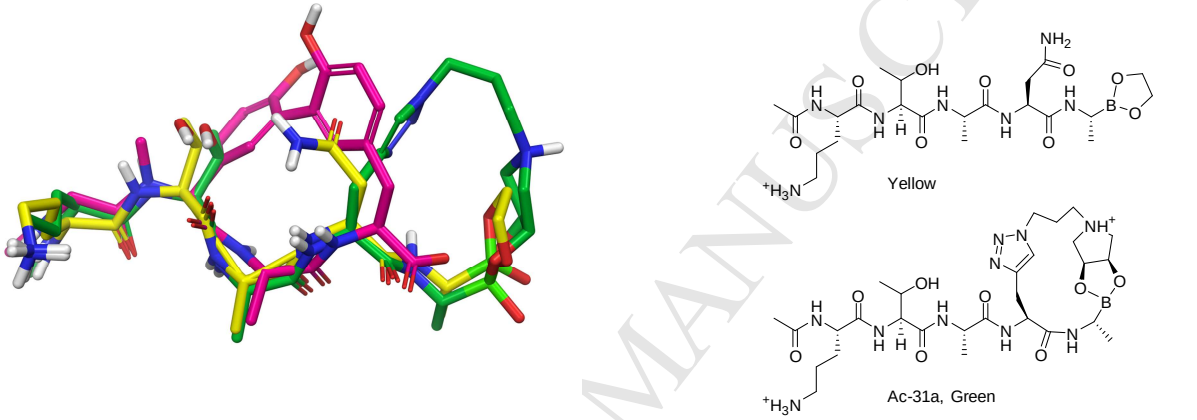

Figure 2. Comparison of the binding conformation of arylomycin A2 (left pane, tail not shown) as observed in the crystal structure (PDB entry: 3IIQ,[36] pink), the modelled *N*-acetylated analogue of the macrocyclic compound **31a** (green), and an *N*-acetylated linear analogue of compound **31a** with an ethylene glycol boronic ester (yellow).

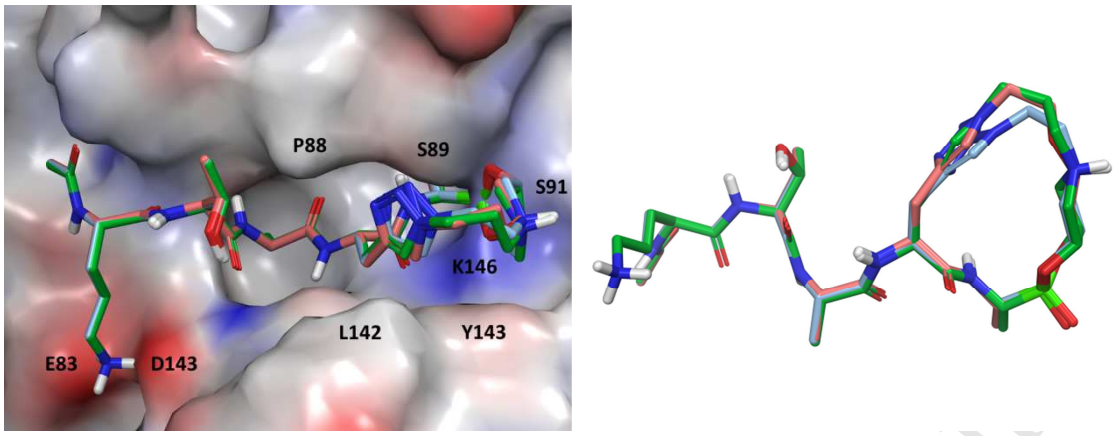

Figure 3. A) Two views of modeled binding conformations of the three designed macrocycles covalently attached to S91 in *Ec*LepB (PDB entry: 3IIQ) (the numbering system for the protein has been adjusted to reflect the corrected sequence reported by Paetzel *et al.* [37]).

2.2 Chemistry

Tetrapeptides **3a-d** were synthesized by manual solid-phase peptide synthesis (SPPS) on 2-chlorotritylchloride (2-CTC) polymer resin using standard protocols for N-terminal 9-fluorenylmethyloxycarbonyl-protected amino acids (Fmoc-AA-OH) solid-phase peptide synthesis as described in the experimental chemistry section (Scheme 1).

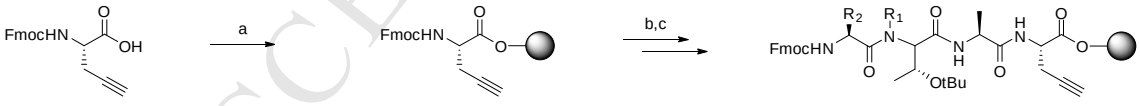

1 **2** **3a-d**

Cmpd	R_1	R_2
3a	H	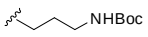
3b	Me	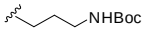
3c	H	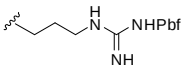
3d	H	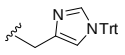

Scheme 1. Solid-phase synthesis of tetrapeptides **3a-d**. *Reagents and conditions*: a) 2-CTC**,** DIEA, DCM, r.t., 2 h, then MeOH, r.t., 0.5 h; b) 20% piperidine in DMF, twice, 5 min + 20 min, r.t.; c) Fmoc-AA-OH, HBTU, DIEA, DMF, r.t., 4 h or 2 h + 2 h double-coupling or overnight.

Synthesis of heteroaromatic tails is depicted in Scheme 2. Compound **6** was prepared *via* Suzuki coupling of methyl 6-bromo-nicotinate with (4-butylphenyl)boronic acid, followed by hydrolysis of the ester. The *N*-aryl pyridone tail **9** was prepared from the corresponding 2-pyridone derivative and (4-hexylphenyl)boronic acid using a process similar to that reported earlier [38]. The octynylnicotinic acid tail **12** was synthesized using standard Sonogashira coupling of ethyl 5-bromonicotinate with 1-octyne, followed by alkaline hydrolysis of the ester. The benzimidazole tail **15** was synthesized by formylation of hexylbenzene using hexamethylenetetramine in trifluoroacetic acid (TFA). In the second step, the resulting crude aldehyde was condensed with 3,4-diaminobenzoic acid in the presence of sodium pyrosulfite to afford the final compound. Compound **18** was made *via* iodination of methyl 1H-indole-5-carboxylate with iodine in the presence of potassium carbonate, followed by Boc protection under standard conditions. Suzuki coupling with (4-hexylphenyl)boronic acid and subsequent lithium hydroxide (LiOH) hydrolysis afforded the required indole tail **20**. The biphenylpropiolic acid tail **23** was synthesized by coupling of ethyl propiolate to biphenyl boronic acid in the presence of copper(I) iodide and silver(I) oxide as described earlier [39], followed by ester hydrolysis.

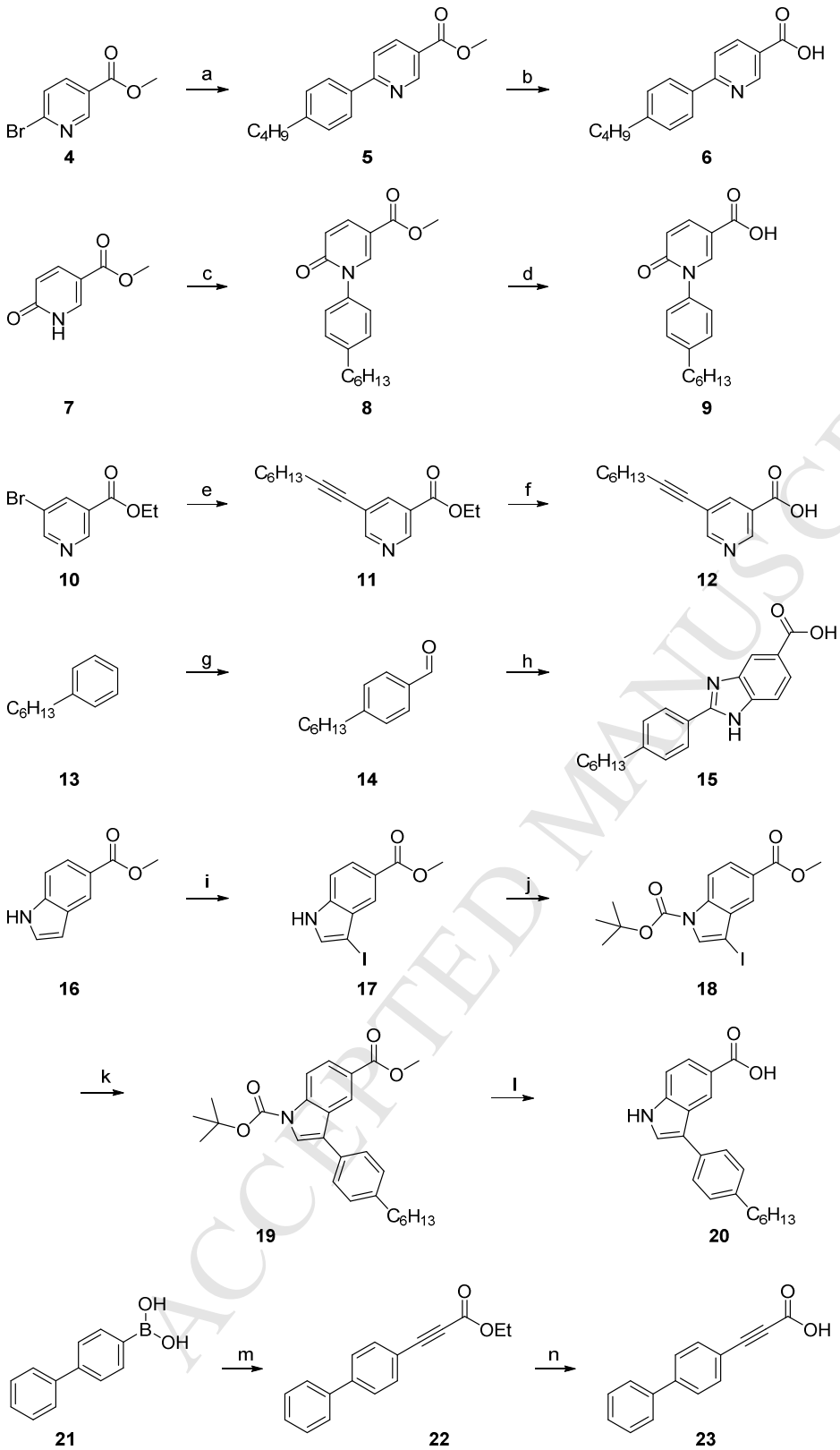

Scheme 2. Synthesis of the heteroaromatic tails. *Reagents and conditions:* a) (4-butylphenyl)boronic, $Pd(PPh_3)_4$, Na_2CO_3, toluene/EtOH/H_2O 3:1:2.5, 110 °C, microwave irradiation, 40 min; b) NaOH, THF/H_2O 5:1, reflux, 2 h; c) (4-hexylphenyl)boronic acid, $Cu(OAc)_2$, Py, mol. sieves, DCM, r.t., 20 h; d) LiOH, THF/MeOH/ H_2O 3:2:1, r.t., overnight;

e) 1-octyne, bis(triphenylphosphine) palladium(II) dichloride, copper(I) iodide and diethylamine in DMF; 50 °C, 15 min; f) $LiOH \cdot H_2O$ in dioxane/H_2O, r.t., overnight; g) hexamethylenetetramine, TFA, 75 °C, overnight; h) 3,4-diaminobenzoic acid, sodium pyrosulfite, DMF, 100 °C, 16 h; i) I_2, K_2CO_3, DMF, r.t., overnight; j) Boc_2O, DMAP, THF, r.t., 1 h; k) (4-hexylphenyl)boronic acid, K_2CO_3, toluene/MeOH 1:1, $Pd(PPh_3)_4$, 75 °C, 40 min; l) $LiOH \cdot H_2O$, THF/MeOH/H_2O 3:2:1, r.t., overnight; m) ethyl propiolate, CuI, Ag_2O, $CsCO_3$, DCE, 80 °C, 24 h; n) $LiOH \cdot H_2O$, THF/MeOH/H_2O 3:2:1, r.t., 1 h.

Coupling of the tail at the N-terminus of the synthesized tetrapeptides **3a-d** was performed using 4'-hexyl-biphenyl-carboxylic acid or 6-(4-butylphenyl)nicotinic acid **6**, giving intermediates **24a-e** (Scheme 3). The final oligopeptides **25a-e** were cleaved from the solid support using a solution of 1,1,1,3,3,3-hexafluoro-2-propanol (HFIP)/DCM (1:4).

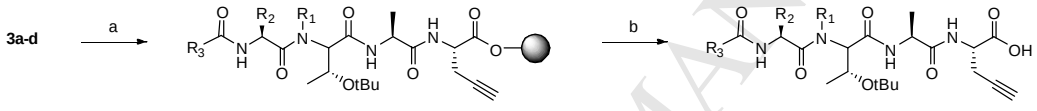

Cmpd	R1	R2	R3
25a	H	NHBoc	I
25b	Me	NHBoc	I
25c	H	NHPbf	I
25d	H	NTrt	I
25e	H	NHBoc	II

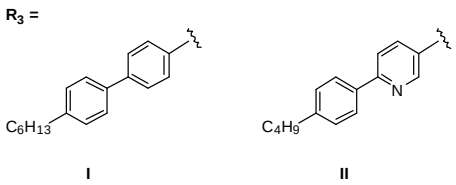

Scheme 3. Synthesis of oligopeptides **23a-e** and **24a**. *Reagents and conditions*: a) RCOOH, HBTU, DIEA, DMF, r.t., 18 h; b) HFIP/DCM 1:4, r.t., 1 h.

To synthesize **28a** and **28b** required for the Click reaction with propargylic peptides **25a-e**, *cis*-pyrrolidine-3,4-diol was protected using a solution of *p*-toluenesulfonic acid in benzaldehyde dimethyl acetal (Scheme 4) [40]. The resulting acetal was *N*-alkylated with 1-bromo-3-chloro-propane or 1-bromo-2-chloro-ethane in the presence of potassium carbonate.

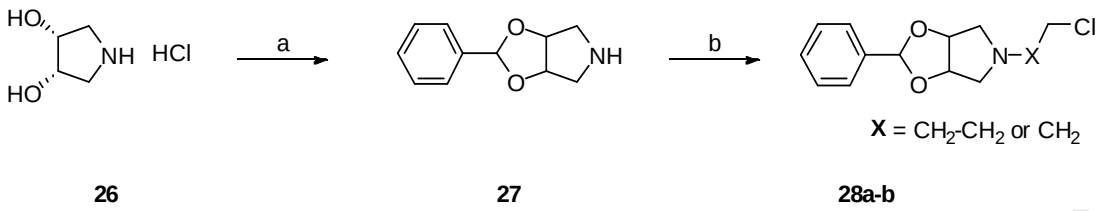

26 **27** **28a-b**

Scheme 4. Synthesis of the chloroalkyl derivatives of *cis*-pyrrolidine-3,4-diol. *Reagents and conditions:* a) benzaldehyde dimethyl acetal, *p*-toluenesulfonic acid, r.t., overnight; b) 1-bromo-3-chloro-propane or 1-bromo-2-chloro-ethane, K_2CO_3, MeCN, 21 h.

The copper(I)-catalyzed azide-alkyne cycloaddition (CuAAC) [41] between the propargylic peptides **25a-e** and azides, generated *in situ* by reaction of sodium azide with the corresponding alkyl halides **28a** and **28b**, afforded the triazole derivatives **29a-f** (Scheme 5). Next, coupling of (*R*)-boroAla-(+)-pinanediol at the C-terminus, followed by complete deprotection with TFA/DCM 1:1 mixture at elevated temperature resulted in transesterification of pinanediol with *cis*-pyrrolidine-3,4-diol to give the final cyclic boronic ester peptides **31a-e**. Structure elucidation studies by NMR revealed partial epimerization during the (*R*)-boroAla-(+)-pinanediol coupling step. Such a racemization occurring via a 5(4H)-oxazolone intermediate is a well-established side effect of carboxyl activation [42,43]. The resulting epimers could not be separated by any HPLC method used and so the compounds were submitted for testing as 1:2 mixtures.

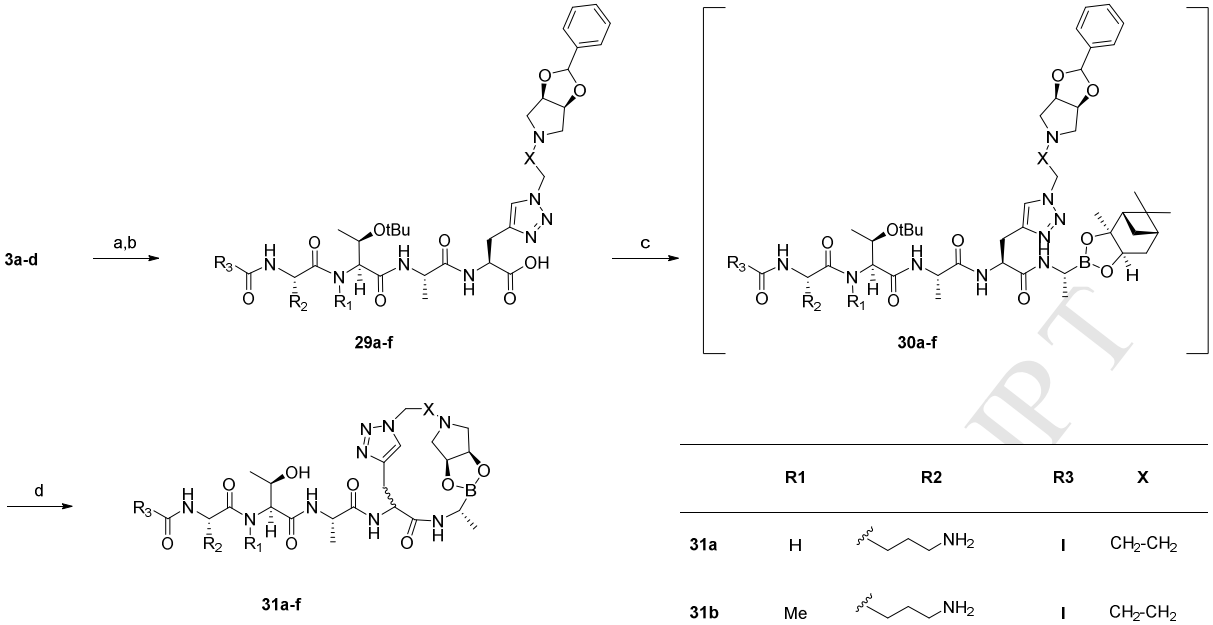

	R1	R2	R3	X
31a	H		I	CH_2-CH_2
31b	Me		I	CH_2-CH_2
31c	H	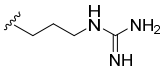	I	CH_2-CH_2
31d	H	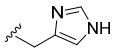	I	CH_2-CH_2
31e	H	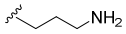	II	CH_2-CH_2
31f	H	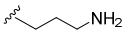	I	CH_2

Scheme 5. Synthesis of peptides **31a-f** with the cyclic boronic ester warheads. *Reagents and conditions:* a) NaN_3, DMF, 60 °C, overnight; b) **25a-e** in H_2O/DMF, Na_2CO_3, copper(II) sulfate pentahydrate, sodium ascorbate, 50 °C, 24 h and r.t., 24 h or 30 °C, 48 h; c) (*R*)-boroAla-(+)-pinanediol hydrochloride, HATU, DIEA, DCM, 0 °C to r.t., 1 h; d) TFA/DCM 1:1, 50 °C, 5 h.

For the preparation of the required cyclopentane-1,2,4-triol moiety **37**, commercially available cyclopentenol **32** was protected using *tert*-butyldiphenylsilyl chloride and sodium hydride (Scheme 6). The resulting olefin was converted to the corresponding diol as described earlier [44] using catalytic amounts of OsO_4 and NMO as re-oxidant via the Upjohn dihydroxylation protocol [45]. In agreement with the previous report, the ratio between *anti*- and *syn*-isomers was approximately 8:1 and the isomers could be separated by column chromatography. The diol was converted into the ketal with 1,3-diphenyl-2-propanone and catalytic amounts of tosylic acid. Subsequent deprotection with TBAF gave the free alcohol **34**. Mitsunobu inversion [46] followed by ester hydrolysis with lithium hydroxide afforded

the corresponding *syn*-alcohol **35.** This was alkylated with *tert*-butyl bromoacetate using sodium hydride as a base and then reduced with $LiAlH_4$ in THF to give pentatriol moiety **36.** Tosylation under standard conditions followed by a nucleophilic substitution with NaN_3 led to the required azide **37**.

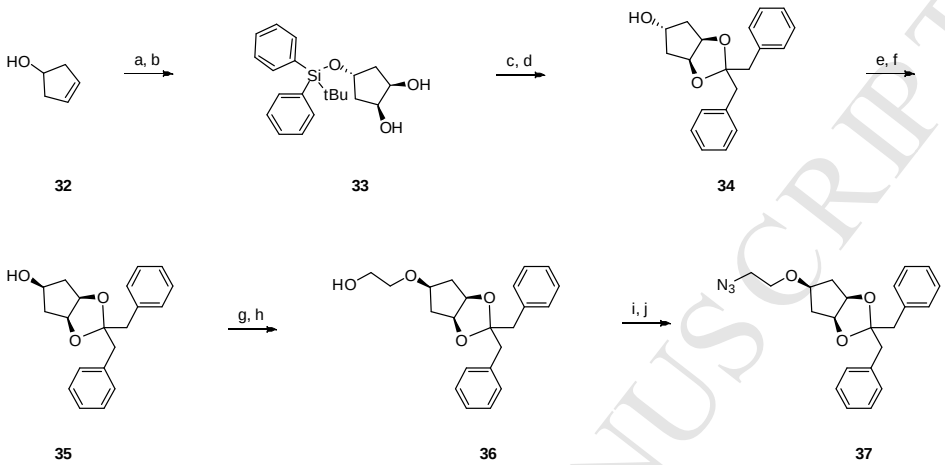

Scheme 6. Synthesis of the protected *syn*-1,2,4-cyclopentanetriol moiety with the azidoethyl linker. *Reagents and conditions*: a) NaH, dry THF, TBDPSCl, 16 h; b) OsO4, NMO, tBuOH/THF/H_2O 3:2:1, r.t., 2 h; c) diphenylacetone, TsOH, DCM, r.t., overnight; d) TBAF, THF, r.t., 1 h; e) p-nitrobenzoic acid, THF, DEAD, r.t., 16 h; f) LiOH, THF/MeOH/water 3:2:1, r.t., 3 h; g) NaH, DMF, *tert*-butyl 2-bromoacetate, r.t., 14 h; h) $LiAlH_4$,THF, r.t., 3 h; i) TsCl, Py, DCM, r.t., 24 h; j) NaN_3, MeCN, 80 °C, 48 h.

Coupling of the commercially available acids (biphenyl-carboxylic acid, 4'-hexyl-biphenyl-carboxylic acid and 6-oxo-1-phenyl-1,6-dihydropyridine-3-carboxylic acid) or the synthesized acids (compounds **9**, **12**, **15**, **20** and **23)** at the N-terminus of the synthesized tetrapeptide **3a** was followed by a solid-phase click reaction between the propargylic group and azide **37.** Cleavage from the solid support gave peptides **40a-h**. The resulting free acids were coupled with *(R)*-boroAla-(+)-pinanediol at the C-terminus; followed by simultaneous deprotection of the side chains and the diol to give the final boronic esters **42a-h**. The lipopeptide **43** used in the NMR studies was prepared using the same protocols as for **42a-h**. Compound **44** was formed from **43** by air-oxidation similar to that described by Snyder *et al.*[47]

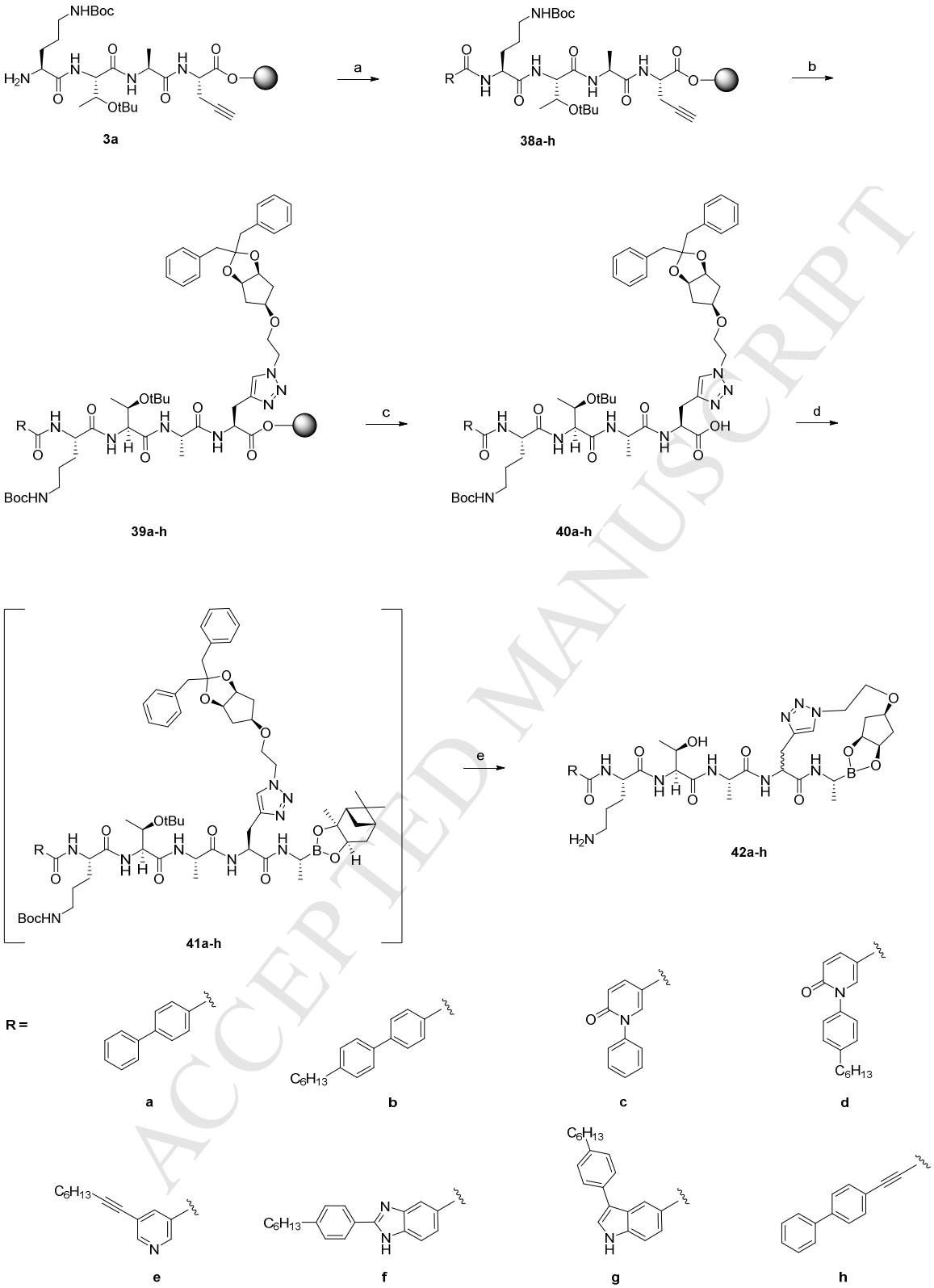

Scheme 7. Synthesis of cyclic boronic ester peptides **42a-h**. *Reagents and conditions*: a) RCOOH, HBTU, DIPEA, DMF, r.t., overnight; or RC(O)OC(O)OtBu, DIPEA, DMF, r.t., overnight; b) azide **36**, copper(II) sulfate pentahydrate, sodium ascorbate, THF/water 3:1, r.t.,

overnight; c) HFIP in DCM (1:4), r.t., 2 h; d) (*R*)-boroAla-(+)-pinanediol hydrochloride, HATU, DIPEA, DCM, 0 °C, 1h; e) TFA/DCM 1:1, 45 °C, 2h.

3. Results and discussion

3.1. In vitro biology

To test *in vitro* potency against *Ec*LepB, we used a previously described FRET-based assay [31]. The measured IC_{50} values (nM) for compounds **31a-f** (esters with a *cis*-pyrrolidine-3,4-diol moiety), **31g-h** (linear reference compounds, see Supplementary data for details**)** and **42a-h (**esters with *all-cis* cyclopentane-1,2,4-triol moiety) are given in Tables 1 and 2, respectively.

In vitro antibacterial activity was determined against seven Gram-negative bacterial strains, including three strains of *Escherichia coli* (WT, efflux-defective and drug-hypersensitive), two strains of *Pseudomonas aeruginosa* (WT and efflux-defective), *Klebsiella pneumoniae* and *Acinetobacter baumannii*. *Staphylococcus aureus* was used as a Gram-positive reference. The results are given as MICs (µg/mL) in Tables 1 and 2.

All of the synthesized compounds were also evaluated on the HepG2 cell line for cytotoxicity using a fluorometric microculture cytotoxicity assay (FMCA) [48] and for hemolytic activity on human blood (see Tables 1 and 2).

3.1.1. Effects of macrocyclization on enzyme inhibition

Comparing the homologous macrocycles **31a**, **31f**, and **42b** (*Ec*LepB IC_{50}s = 105, 104, and 175 nM, respectively) with the linear reference analogue **31h** having an asparagine in P2 and a boronic acid pinanediol ester (*Ec*LepB IC_{50} = 17 nM), it can be seen that the macrocyclization slightly decreases the potency of enzyme inhibition. If this is an effect of the macrocyclization *per se* or a consequence of the difference in P1' and/or P2 is difficult to say. However, as was expected from modeling, the minor variations in the macrocycle in positions facing solvent had no dramatic impact on enzyme inhibition. Thus, this part of the molecule can be used for modulating bacterial penetration and ADMET properties.

3.1.2. Arginine and histidine in P5 and N-methylation in P4 to reduce cytotoxicity

As both **31a** and **31f** showed cytotoxicity against HepG2 cells (Table 1), we considered changes in P5 to alleviate this issue. Sosic *et al.* [49] have reported that replacing an aminoethyl group with an guanidinoethyl group could provide a reduction of non-specific cytotoxicity. We therefore synthesized two variants in P5 carrying arginine (**31c**) and histidine

(**31d**) instead of ornithine. As was expected from the modeling, since the P5 side chain is solvent-exposed, both compounds were potent inhibitors of LepB with IC_{50} values similar to those of **31a** and **31f**. Compound **31c** with arginine in P5 was clearly best, in terms of inhibition (*Ec*LepB IC_{50} = 41 nM) and antibacterial activities, but unfortunately, it was worse in terms of cytotoxicity and hemolysis. The less basic P5 histidine substitution (**31d**), although active on the enzyme, was completely inactive in the MIC assay, and did not fare well in the cytotoxicity and hemolysis assays.

N-methylation can modulate the properties of peptides, and so a P4 *N*-methylated compound (**31b**) was also synthesized. Although this was tolerated from an enzyme inhibition perspective, there was a significant loss in terms of MIC. In addition, the methylation did not have any dramatic effect on either cytotoxicity or hemolysis.

3.1.3. Replacing cis-pyrrolidine-3,4-diol by all-cis cyclopentane-1,2,4-triol to reduce charge

A major challenge with compounds **31a-d** and the smaller macrocyclic inhibitor **31f** was clearly their hemolytic properties. It is known that reducing the number of positive charges on amphipathic compounds can reduce hemolysis [50]. Therefore, we designed a new macrocyclic scaffold where the basic pyrrolidine was replaced by a neutral cyclopentyl group linked to P2 by an ether linkage. Although the resulting macrocycle **42b** showed a two-fold reduction in *Ec*LepB inhibition (IC_{50} = 175 nM) compared to the two other macrocyclic variants (compounds **31a** and **31f**), it was twice as good in terms of its antibacterial activity. Compared to the equal-sized pyrrolidine based compound **31a** the level of hemolysis was halved for the ether analogue **42b** (10.6%, see Table 2) and the cytotoxicity was reduced.

3.1.4. Increasing polarity of the tails to reduce cytotoxicity

Inspired by the work on polymyxin analogues by Magee *et al.* [51], where more polar tails resulted in reduced cytotoxicity, a number of different tails, including truncated versions, were introduced (compounds **31e** and **42c – 42g**, see Tables 1 and 2). From the results, it can be concluded that the aliphatic part of the lipophilic tail is not the major driver for enzyme inhibition (Table 2). Comparing, for example, **42a** (biphenyl, IC_{50} = 72 nM) with **42b** (hexylbiphenyl; IC_{50} = 175 nM), and **42c** (1-phenylpyridin-2-one; IC_{50} = 1660 nM) with **42d** (1-(4-hexylphenyl)pyridin-2-one; IC_{50} = 495 nM), it is clear that the hexyl chain only marginally affects the enzyme inhibition. However, the length/lipophilicity of the tail is crucial for the antibacterial activity, as shown by a lack of MIC activity for the truncated analogues **42a** and **42c**.

With regard to the heteroaromatic tails (see Tables 1 and 2), the lipophilicity of these was in general significantly reduced, with the exception of **42f** and **42g**, which were synthesized to incorporate hydrogen-bond donors. Two of the less hydrophobic tails, 6-(4-butylphenyl)nicotinyl (**31e**) and the elongated 5-(oct-1-yn-1-yl)nicotine (**42e**) were well-tolerated in terms of enzyme inhibition, whereas the bent pyridin-2-one based compounds (**42c** and **42d)** were less potent. Compound **42g**, geometrically similar to the latter, was less potent in terms of enzyme inhibition. In the case of 2-(4-hexylphenyl)-1H-benzo[d]imidazole (**42f**), we observed an improvement in the *Ec*LepB inhibition, with this compound being the most potent inhibitor in the current study (IC_{50} = 29 nM).

Although all of these compounds were active in terms of enzyme inhibition, all changes to the lipophilic tail resulted in increased MIC values. Only **42g**, the indole derivative, had any appreciable antibacterial properties, but still was appreciably worse than **42b**. In terms of cytotoxicity and hemolytic properties, the less lipophilic compounds, **31e**, **42a**, **42c**, **42d**, and **42e** were, however, superior to **42b**. Clearly, the separation of antibacterial properties and toxicity is a significant challenge for lipopeptides targeting *Ec*LepB.

Table 1

Inhibition potency against *Ec*LepB, antibacterial activity, cytotoxicity and hemolysis for macrocyclic boronic esters **31a-h** with a *cis*-pyrrolidine-3,4-diol moiety.

cmpd	structure	*Ec*LepB IC_{50} (nM)[a]	MIC (µg/mL)								Cytotoxicity IC_{50} (µM)[j]	Hemolysis (%)
			E. c.[b]	E. c.[c]	E. c.[d]	P. a.[e]	P. a.[f]	K. p.[g]	A. b.[h]	S. a.[i]		
31a	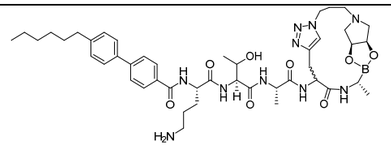	105 (68-162)	32	8	8	> 64	64	32	16	32	4.0	17.4 ± 1.1
31b	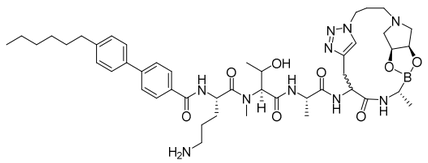	98 (59-159)	64	16	32	> 64	64	32	64	32	8.5	9.6 ± 1.8
31c	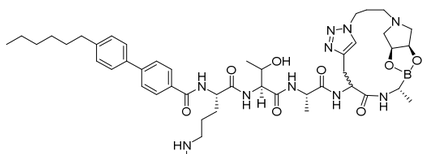	41 (31-52)	16	4	8	> 64	32	16	16	16	2.4	21.0 ± 2.9
31d	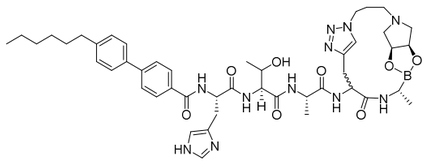	107 (84-136)	> 64	> 64	64	> 64	> 64	> 64	> 64	> 64	5.4	4.1 ± 0.2
31e	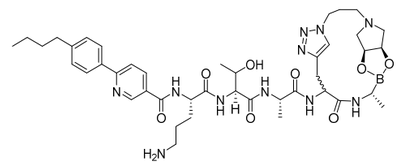	42 (34-51)	> 64	32	64	> 64	> 64	> 64	> 64	32	29.1	7.3 ± 0.5
31f	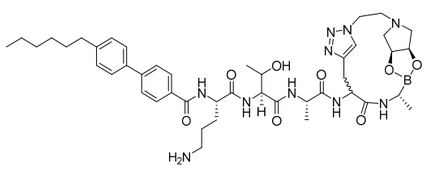	104 (77-141)	64	16	32	> 64	> 64	64	32	32	9.5	10.1 ± 1.1
31g	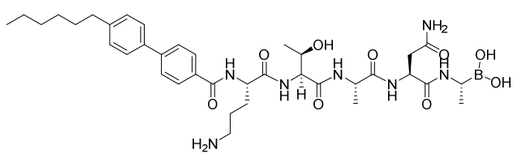	52 (38-71)	8	1	0.5	64	16	2	4	0.025	10.1	4.8 ± 0.4

31h	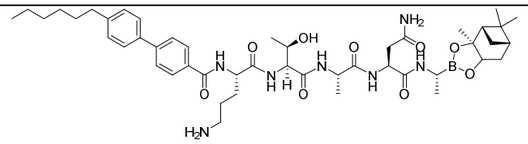	17 (16-18)	8	2	0.5	64	32	2	4	0.025	11.7	11.7 ± 0.8

[a]95% Confidence interval is shown in parentheses; [b]*E. coli* ATCC 25922 WT; [c]*E. coli* ΔtolC (CH3130, efflux-defective mutant isogenic to ATCC 25922); [d]*E. coli* D22 (CGSG 5163, lps mutant, drug-hypersensitive); [e]*P. aeruginosa* PAO1 WT; [f]*P. aeruginosa* efflux-defective PAO750 (isogenic to PAO1); [g]*K. pneumoniae* ATCC 13883 WT; [h]*A. baumanii* ATCC 19606 WT; [i]*S. aureus* ATCC 29213 (Gram-positive reference); [j]cytotoxicity of HepG2 cells.

Table 2

Inhibition potency against *Ec*LepB, antibacterial activity, cytotoxicity and hemolysis for macrocyclic boronic esters **42a-h** with a cyclopentane-1,2,4-triol moiety.

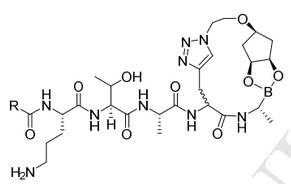

			MIC (µg/mL)									
cmpd	R	*Ec*LepB IC_{50} (nM)[a]	E. c.[a]	E. c.[b]	E. c.[c]	P. a.[d]	P. a.[e]	K. p.[f]	A. b.[g]	S. a.[h]	Cytotoxicity IC_{50} (µM)[i]	Hemolysis (%)
42a	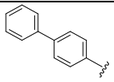	72 (56-93)	> 64	> 64	> 64	> 64	> 64	> 64	> 64	> 64	> 64	0.2 ± 0.3
42b	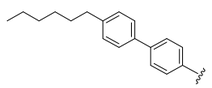	175 (144-213)	16	4	4	64	32	8	8	2	8.0	10.6 ± 1.4
42c	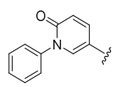	1660 (1060-2590)	> 64	> 64	> 64	> 64	> 64	> 64	> 64	> 64	> 64	0.04 ± 0.01
42d	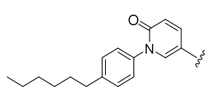	495 (359-683)	> 64	> 64	> 64	> 64	> 64	> 64	> 64	64	> 64	0.03 ± 0.15
42e	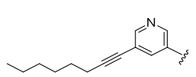	41 (33-52)	> 64	64	> 64	> 64	> 64	> 64	> 64	32	> 64	0.01 ± 0.01
42f	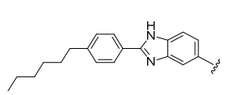	29 (25-34)	> 64	16	64	> 64	64	64	64	4	24.4	0.5 ± 0.2
42g	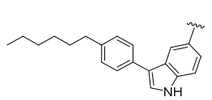	225 (195-261)	32	32	16	64	64	64	64	16	23.7	2.8 ± 0.6

42h	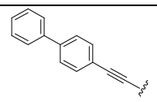	227 (168-305)	> 64	> 64	> 64	> 64	> 64	> 64	> 64	32	28.2	0.01 ± 0.02

[a]95% Confidence interval is shown in parentheses; [b]*E. coli* ATCC 25922 WT; [c]*E. coli* ΔtolC (CH3130, efflux-defective mutant isogenic to ATCC 25922); [d]*E. coli* D22 (CGSC 5163, lps mutant, drug-hypersensitive); [e]*P. aeruginosa* PAO1 WT; [f]*P. aeruginosa* efflux-defective PAO750 (isogenic to PAO1); [g]*K. pneumoniae* ATCC 13883 WT; [h]*A. baumanii* ATCC 19606 WT; [i]*S. aureus* ATCC 29213 (Gram-positive reference); [j]cytotoxicity of HepG2 cells.

3.2. Confirmation of macrocyclization

Macrocyclization of compounds **42a-h** was corroborated by mass spectrometric and NMR analyses of compound **43** (Figure 4). This polyalanine analogue has a simplified structure that enabled unambiguous and quick spectral analyses.

^{1}H NMR assignment was performed using a NOESY-TOCSY backbone walk, and further corroborated by the cross peaks observed in gCOSY, ^{1}H,^{13}C- and ^{1}H,^{15}N-gHSQC, and ^{1}H,^{13}C- and ^{1}H,^{15}N-gHMBC spectra. The spectra were obtained at several temperatures within the 25 °C-80 °C range to support interpretation of overlapping signals (see supplementary data for details). The observed molecular mass $[M+H]^{+}$ 729.3558 (calcd 729.3532 for $C_{36}H_{45}BN_8O_8$), along with the key NOE correlations shown in Figure 4, confirmed ring closure. The latter NOEs were in agreement with the computed cyclic geometry of **43** (Table S1), and none corresponded to its hydrolyzed, ring-opened analogue (Figure 4). The ^{1}H NMR signals of **43** were doubled, and did not coalesce at high temperatures, which revealed it to be a 2:1 mixture of epimers due to partial racemization of the P2 amino acid during the final coupling of the boronic amino acid. It is well known that activation of the C-terminal carboxylic acid of the peptide chain is associated with oxazolone formation that leads to the formation of peptide epimers [42].

The largest chemical shift differences of the epimers were observed for the nuclei of the macrocycle, suggesting that the point of epimerization is H-1' (Figure 4). The amide temperature coefficients of all amide protons of **43** were in the range of 4.0-4.6 ppb/K, suggesting them to be in equilibrium between intramolecularly hydrogen-bonded and solvent-exposed states, apart from those of Ala-1 and P2, whose values of 9.2 ppb/K and 8.1 ppb/K revealed them to be solvent exposed [52,53]. The latter are most likely unavailable for intramolecular hydrogen bonding due to their participation in the macrocycle. Upon hydrolysis to **44**, the amide temperature coefficient of P2 decreased to 3.8 ppb/K, and hence this group became available for intramolecular hydrogen bonding during the opening of the macrocycle and the consequent major structural change.

Furthermore, the computed cyclization free energies given in Table S1 predict that the ring-closed forms of the macrocycles are stable towards hydrolysis in DCM, DMSO and water.

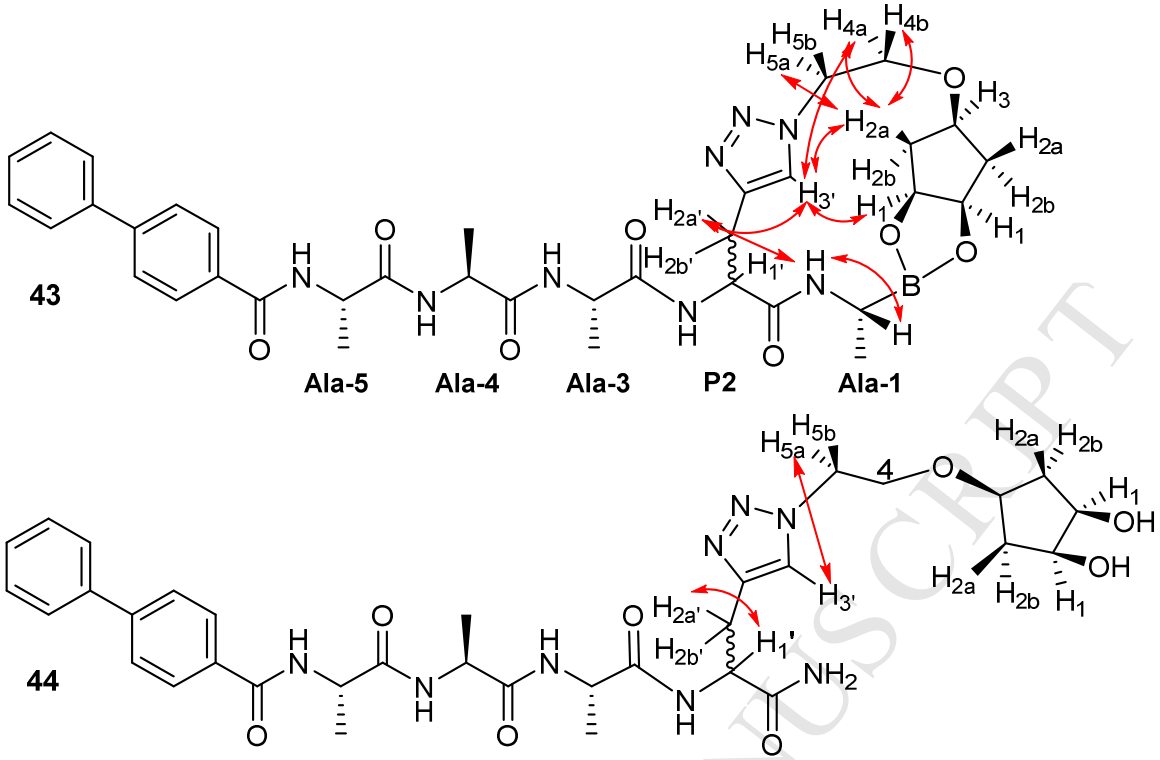

Figure 4. The cyclic peptide **43** (IC_{50} 18 nM; MIC > 64 µg/mL on all strains) and the linear peptide **44** used for NMR confirmation of macrocyclization, with the key NOE information being shown as red arrows.

4. Summary and conclusions

This project was initiated in response to the observed cytotoxic and hemolytic liabilities among previously studied linear lipopeptide boronic acids and esters[31]. We have designed and synthesized first-in-class P2–P1' boronic ester-linked macrocycles. This extends the chemical space available for designing *Ec*LepB inhibitors, allowing more options for tuning the properties of the boronic ester warhead, and potentially leading to potent *Ec*LepB inhibitors with improved antibacterial activity and *in vitro* toxicity profiles.

Ultimately, 14 novel macrocyclic lipopeptides differing in the macrocyclic linker, the peptide sequence and in the lipophilic tail were synthesized to investigate the structural requirements for enzyme inhibition, antibacterial activity and toxicity. MS and NMR analyses provided the macrocycle to exist in the ring-closed form. Good enzyme inhibition and MIC data showed that the macrocyclization was indeed tolerated by the enzyme. Macrocyclization via an ether linkage, as in **42b,** resulted in a compound active against all strains in the antibacterial panel, including wild types.

Cytotoxicity and hemolysis remained highly correlated with antibacterial activity. For the macrocyclic *Ec*LepB inhibitors having MIC activities, cytotoxicity and hemolysis remained at the levels observed for the linear analogues. Thus, striking the right balance between the total charge of the peptide, the composition and length of the hydrophobic tail, the overall hydrophobicity and amphipathicity resulting in more effective and safe *Ec*LepB inhibitors remains an important challenge when targeting this enzyme.

To conclude, we have demonstrated that the P2 to P1' linker can provide a means for future optimization of the properties of *Ec*LepB inhibitors. We also envision that P2–P1' boronic ester-linked macrocycles can be of general use against other proteases.

5. Experimental section

5.1. Chemistry

5.1.1. General methods

Analytical thin layer chromatography (TLC) was performed using Merck aluminum sheets precoated with silica gel 60 F_{254}. Column chromatography was performed on Merck silica gel 60 (40-63 μm). The microwave reactions were performed in a Biotage Initiator producing controlled irradiation at 2450 MHz with a power of 0–300 W. ^{1}H and ^{13}C NMR spectra were recorded on Varian Mercury Plus instruments; ^{1}H at 399.9 MHz and ^{13}C at 100.6 MHz at 25 $^{\circ}C$. Exact molecular masses were determined on Micromass Q-Tof2 mass spectrometer equipped with an electrospray ion source. Analytical RP-HPLC-MS was performed on a Gilson RP-HPLC system with a Finnigan AQA quadrupole low-resolution mass spectrometer in positive or negative ESI mode using a Onyx Monolithic C_{18} 4.6 × 50 mm 5 μm (Phenomenex) with MeCN in 0.05% aqueous HCOOH as mobile phase at a flow rate of 4 mL/min. Preparative RP-HPLC was performed on a system equipped with a Nucleodur C18 HTec 5 μm column (150 × 21.2 mm) or a Phenomenex C8 5 μm column (150 × 21.2 mm), using a H_2O/CH_3CN gradient with 0.1% TFA or H_2O/CH_3CN gradient with 20 mM TEAA, in both cases using UV detection at 220 nm and 254 nm. The purity of the peptides was determined by RP-HPLC using the columns: ACE 5 C18 (50 × 4.6 mm) and Nucleodur C18 HTec 5 μm (4.6 × 50 mm), H_2O/CH_3CN gradient with 0.1% TFA or H_2O/CH_3CN gradient with 20 mM TEAA and UV detection at 220 nm and 254 nm. All peptides showed purity above 95%.

5.1.2. General method for solid phase synthesis of oligopeptides

Tetrapeptides **3a-d** were synthesized by manual solid-phase peptide synthesis (SPPS) using 2-chlorotritylchloride polymer resin (2-CTC, 1.63 mmol/g) in a 10-mL disposable syringe fitted with a porous polyethylene filter and N-terminal fluorenylmethyloxycarbonyl-protected amino acids. Coupling of the first amino acid: Fmoc-propargyl-Gly-OH (0.8 eq.) to the 2-CTC resin (1.0 eq.) was performed in anhydrous DCM (7.5 mL) in the presence of DIEA (3.0 eq.) with shaking at room temperature for 2 h. Then, MeOH (2 mL) was added to cap the unreacted resin and the mixture was shaken for 30 min. The resin was filtered, washed with several portions of DCM, DMF and again DCM and dried under high vacuum, overnight. Loading of the starting material was calculated *via* increase in dry weight. Next, the resin swelling was performed in DMF for 20 min, Fmoc protecting group was removed by treatment with 20% piperidine in DMF (2 × 3 mL, 5 + 20 min) and the polymer was washed with DMF (5 × 3 mL, 5 × 2 min). Then, coupling of the appropriate amino acid: Fmoc-AA-OH (4.0 eq.) was performed in DMF (3 mL) using HBTU (4.0 eq.), in the presence of DIEA (8.0 eq.) with shaking at room temperature. In the case of Fmoc-Ala-OH for 4 h, with Fmoc-Orn(Boc)-OH, Fmoc-Thr(*t*Bu)-OH and Fmoc-*N*-Me-Thr(*t*Bu)-OH overnight and with Fmoc-Arg(Pbf)-OH and Fmoc-His(Trt)-OH the double coupling was performed (after 2 h the resin was washed with DMF and treated with a freshly made solution of Fmoc-AA-OH, HBTU and DIEA in DMF and shaken for 2h). After each coupling, the resin was washed with DMF (4 × 4 mL) and subsequently de-protected and washed as described above. At the end of the coupling cycle the resin was washed with several portions of DMF, MeOH and DCM and dried under high vacuum, overnight. Method (A) for coupling of the tailDMF via HBTU activation. The coupling of the tails at the N-terminus of the synthesized tetrapeptides was performed using the acid (4 eq.) in DMF (2 mL), in the presence of DIEA (8 eq.) and HBTU (4 eq.) at room temperature, shaking overnight. The resin was then washed extensively with several portions of DMF, MeOH and DCM and dried under high vacuum. Method (B) for coupling of the tail via mixed anhydride. Step 1. Heterocyclic acid derivative (0.520 mmol, 1 eq.) was reacted with Boc anhydride (2.110 mmol, 4 eq.) in dry tetrahydrofuran in presence of pyridine (2.640 mmol, 5 eq.) at r.t. overnight. After full consumption of starting material volatiles were removed *in vacuo*. Aqueous 0.5M hydrochloric acid solution was added and the product was extracted with ethyl acetate. The organic layer was washed with water, separated and dried over sodium sulfate. Volatiles were removed *in vacuo* yielding a crude product as yellowish oil, which was used in the next step without further purification. Step 2. The 2-CTC resin containing **3a** (0.130 mmol, 1 eq.) was suspended in DMF (3 mL) containing mixed

anhydride prepared in Step 1 (presumed 0.52 mmol, 4 eq.) and DIPEA (1.820 mmol, 14 eq.). The reaction mixture was shaken at r.t. overnight. The resin was filtered, washed with DMF (5 x 2 mL), DCM (5 x 2 mL) and THF (5 x 4 mL). General method for cleavage from the solid support. 2-CTC resin containing oligopeptides was added into a mixture of HFIP/DCM 1:4 (4 mL) and the reaction mixture was shaken at room temperature for 1.5 h. The resin was filtered off and washed with DCM and THF. The volatiles were evaporated *in vacuo*. Purification. The crude peptides were dissolved in THF (2.5 mL) and H_2O/MeCN (1:1, 2.5 mL), filtered through a 0.45 µm nylon membrane filter and purified in 1-3 runs by preparative RP-HPLC. The reported yields are based on calculated loading of the oligopeptide on 2-CTC resin.

5.1.3. General method for the copper(I)-catalyzed azide-alkyne cycloaddition in solution

To a solution of the alkyl chloride **28a** or **28b** (1.3 eq. or 1.5 eq.) in DMF, sodium azide (2.6 eq. or 3.0 eq.) was added. The reaction mixture was stirred at 60 °C overnight. Then, peptide **25a-e** (1.0 eq.) in H_2O/DMF 1:3, Na_2CO_3 (3 eq.), sodium ascorbate (0.8 eq.) and $CuSO_4 \cdot 5H_2O$ (0.4 eq.) were added and stirred at 50 °C or 60 °C for 24 h and at r.t. for 24 h or at 30 °C for 48 h. The reaction mixture was filtered through a 0.45 µM nylon membrane, diluted with H2O/MeCN (1:1) and purified by preparative RP-HPLC.

5.1.4. General method for the copper(I)-catalyzed azide-alkyne cycloaddition on the solid phase

2-CTC resin containing bound oligopeptides **38a-h** (0.130 mmol, 1 eq.) was mixed with THF (1.8 mL) containing azide **37** (0.140 mmol, 1.1 eq.). In a separate vial sodium ascorbate (0.140 mmol, 1.1 eq.) was dissolved in water (0.900 mL). To this solution copper sulfate was added (0.060 mmol, 2.3 eq.), which quickly generated brown solution. The resulting solution was immediately taken into the reactor containing oligopeptide and azide. The reaction mixture was shaken at r.t. overnight. Then, the resin was filtered, washed with DMF (3 x 5 mL), H_2O (3 x 5 mL), THF (3 x 5 mL) and DCM (3 x 5 mL).

5.1.5. General method for the coupling of oligopeptides with R-(+)-boro-Ala-pinanediol and for side chain deprotection and cyclization

To a solution of the peptide (1 eq.) in anhydrous DCM (10 mL) HATU (2 eq.) and DIEA (3 eq.) were added under nitrogen atmosphere at 0 °C and the reaction mixture was stirred at 0 °C for 6 min, then *R*-(+)-boro-Ala-pinanediol (2 eq.) was added and the reaction mixture was

stirred at room temperature for 1h. To the DCM solution of crude peptide generated in *R*-(+)-boro-Ala-pinanediol coupling step (1 eq.) TFA was added to a final ratio of TFA/DCM 1:1. The resulting mixture was stirred at 50 °C for 5 h. The solvents were removed under reduced pressure and the residue was purified by preparative RP-HPLC.

5.2. Computational details

All calculations were performed within the Schrödinger Small-Molecule Drug Discovery Suite 2017-1 using the OPLS3 force field.[54] The crystal structure of LepB from *E. coli* was downloaded from the Protein Data Bank [55] (PDB entry: 3IIQ) and thereafter prepared using the Protein Preparation Wizard [56] implemented in Maestro [57] using default settings. This included addition of hydrogens, hydrogen-bond network optimization, removal of water molecules forming less than three hydrogen bonds to non-waters and a restrained minimization. To evaluate if macrocycles cyclized between the boronic acid and P2 could fit into the LepB binding pocket and interact with the protein in a similar way as arylomycin, the macrocyclic compounds were built into the active site manually using the protein-bound conformation of arylomycin as a template. This was done by adding an *(R)*-boro-alanine to arylomycin which was attached covalently to S91 in the protein, exchanging the side-chains of arylomycin to an Orn-TANA sequence, deletion of the remaining amino acids, truncating the lipophilic tail to an acetyl group and converting the boronic acid to an ethylene glycol boronic ester. The resulting complex was refined using 1 000 steps of MCMM conformational sampling in a GB/SA continuum solvation model for water. The boronate ester and protein side chains within 5 Å from the boronic-peptide were sampled. Protein backbone and amino acids more than 5 Å away from the boronate ester were kept frozen. The resulting binding mode was consistent with the previously published modeling of a similar linear peptide boronic acid [31]. Using the refined structure, seven macrocycles with linker lengths varying between 2-5 and 2-4 carbon atoms between amine-tetrazole and ether-tetrazole were built, respectively. To evaluate if the peptides still could adopt the arylomycin backbone conformation after macrocyclization, the protein-macrocycle complexes were refined using 5 000 steps MCMM conformational sampling and a GB/SA continuum solvation model for water. Side chains within 5 Å of the macrocycles were free to move but not sampled. The protein backbone and side chains more than 5 Å away from the macrocyclic compound were kept frozen.

5.3. EcLepB inhibition assay

In *vitro* potency against *Ec*LepB was determined using a FRET-based assay as described previously. Briefly, the peptide substrate included Dabcyl as the fluorescence acceptor, and EDANS as the donor, attached to the termini (i.e. Dabcyl-VGGTATA↓GAFSRPGLE(EDANS)-OH). After pre-incubation of *Ec*LepB (estimated 50 nM) with synthesized compounds for 10 min, the reaction was initiated with substrate (final concentration 8 μM; K_m 20 μM), and the increasing fluorescence intensity was monitored continuously at 535 nm at 22 °C for 2 h. Cleavage rates were plotted as a function of inhibitor concentration, and non-linear regression analysis of the sigmoidal dose-response curves was employed to calculate half-maximal inhibitory concentration (IC_{50}) in CDD (https://www.collaborativedrug.com).

5.4. Minimal inhibitory concentration (MIC) assay

Compounds were evaluated against a panel of Gram-negative bacteria, including: *E. coli* ATCC 25922, wild-type; CH3130, an efflux-defective ΔtolC mutant isogenic to ATCC 25922; D22, a drug-hypersensitive *lpxC* mutant of *E. coli*; *P. aeruginosa* PAO1, wild-type; PAO750, an efflux-defective mutant isogenic to PAO1; *K. pneumoniae* ATCC 13833, wild-type; *A. baumannii* ATCC 19606, wild-type; and the Gram-positive *S. aureus* ATCC 29213, wild-type. *In vitro* antimicrobial activity of each compound was determined by measuring the MIC value using the broth micro-dilution technique in cation-adjusted Mueller-Hinton II medium (Becton-Dickinson, 212322) according to EUCAST and CLSI guidelines. Compound prepared in MHII medium was dispensed into a 96-well round-bottomed microtiter plate to give final assay concentrations from 64 μg/mL down to 0.25 μg/mL (two-fold dilution series in 10 wells, plus two control wells: medium control with no bacteria or compound, and growth control with bacteria added but no compound). Bacteria prepared from fresh colonies (grown on non-selective agar, incubation 18-24 h at 35 °C ± 2 °C) were suspended in saline to 0.5 McFarland (≅ 1.5×10^8 CFU/mL). 50 μL of this bacterial suspension was transferred to 10 mL of MHII broth to give a final bacterial concentration ≅ 5×10^5 CFU/mL (acceptable range $3 – 7 \times 10^5$ CFU/mL)**.** 50 μL of bacterial suspension was pipetted into each well (except the medium control well, where 50 μL MHII was pipetted). Final volume in each well was 100 μL. Plates were covered and incubated without shaking for 16-20 h at 35 °C ± 2 °C. MIC

was read visually, as complete inhibition of growth by the unaided eye, using the medium-only wells as the control.

5.5. Cytotoxicity assay

Cytotoxicity was assessed in HepG2 cells using fluorometric microculture cytotoxicity assay (FMCA) [48]**.** The cell line HepG2 was obtained from ATCC, and cultured in Eagle's Minimum Essential Medium (ATCC) supplemented with 10% fetal bovine serum, penicillin/streptomycin (100 U/100 µg/mL) and L-glutamine 2 mM (all from Sigma St Louis, MO, USA). HepG2 cells were passaged 2 times/week and used maximally for 20 passages. Cells were finally seeded in Nunc 384-well assay plates at a density of 1000 cells/well. The FMCA is based on measurement of fluorescence generated from hydrolysis of fluorescein diacetate (FDA) to fluorescein by cells with intact plasma membranes. HepG2 cells (1000/well) were seeded in 384-well plates using the pipetting robot Biomek 4000 (Beckman Coulter, Fullerton CA, USA) and cultured overnight before inhibitors were added by acoustic dispensing (Echo 550 from Labcyte Inc, CA, USA) directly from 384-well source plates (Labcyte) containing 1 or 10 mM compound stock solutions in DMSO. Each compound was dispensed for dose-response, with eight two-fold dilutions in duplicate from highest concentrations of 64 or 32 µM, to generate IC_{50}s. Bortezomib (2 µM) was used as positive control, and dose response testing of doxorubicin (highest concentration 2 µM) was performed repeatedly to follow assay performance over time. After 72 h incubation with drugs in a culture chamber (at 37 °C, humidity 95%, 5% CO_2) the 384-well plates were centrifuged (200 × g, 60 sec), the culture medium was removed by a Biotech ELX washer (Biotek, Winooski, VT, USA) and 70 µL phosphate buffered saline (PBS, Sigma) was added to the wells. This procedure was repeated once. Subsequently, the plates were centrifuged (200 × g, 30 sec) and the PBS was removed by the ELX washer after which 50 µL/well of assay buffer (HEPES-buffered saline with 0.5 mM $MgCl_2$ and 0.5 mM $CaCl_2$, pH 7.4) was added to the plates using a Multidrop 384 (Thermo Fischer Scientific, NY, USA). Finally, 1 µL of fluorescein diacetate (0.5 mg/mL in DMSO) was added to each well using the pipetting robot Biomek NX (Beckman Coulter, Fullerton CA, USA). The plates were then incubated for 50 min in a Cytomat (37 °C, humidity 95%, 5% CO_2, Thermo Fischer Scientific) before being analyzed in a Fluostar Omega microplate reader (BMG Technologies, Germany) with wavelengths set at 485 nm (excitation) and 530 nm (emission). Cytotoxicity was assessed after 72 h with cell survival presented as survival index (SI, %) defined as fluorescence in test wells in percent of control cultures with blank values subtracted. Criteria for a successful

assay included a signal-to-noise ratio in control cultures > 10, CV < 30% and a positive control (bortezomib) SI of < 5%. The half maximal inhibitory concentration (IC_{50}) was determined from log concentration-effect curves in GraphPad Prism using a non-linear regression analysis.

4.6. Hemolysis assay

Compounds were evaluated for hemolytic activity using red blood cells from heparinized human blood. Red blood cells (RBC) were washed three times in Tyrode buffer (130 mM NaCl, 4 mM KCl, 2.8 mM Na acetate, 1 mM $MgCl_2$, 10 mM HEPES, 10 mM glucose, 1 mM $CaCl_2$, adjusted to pH 7.4) and resuspended in the same buffer. Final concentrations in the hemolysis assay were: 100 μM compound, 1% DMSO, and 50% RBC, assayed in a 200 μL volume in a microtiter plate. The mixture was incubated at 37 °C for 45 min with shaking (250 rpm). After incubation, RBCs were removed by centrifugation (1000 × g for 10 min), 100 μL clear plasma was transferred to a fresh microtiter plate, and the amount of hemoglobin measured using a spectrophotometer at 540 nm. The complete lysis control contained 2% Triton X-100 (in Tyrode buffer) instead of compound; the negative control contained Tyrode buffer but no compound. Percent hemolysis was calculated as: [Abs compound] - [Abs negative control] / [Abs complete lysis control] - [Abs negative control] x 100. Values greater than 1% hemolysis at 100 μM were regarded as a red flag.

Conflict of interest

The authors declare that there is no conflict of interest.

Acknowledgements

This work was supported by the Swedish Research Council (2014-6711, 2015-05406, 2017-03953). We thank Lena Lenhammar and Rolf Larsson for contributing with cytotoxicity data.

REFERENCES

[1] World Health Organization, Antibacterial agents in clinical development, an analysis of the antibacterial clinical development pipeline, including tuberculosis, World Health Organization, 2017.

[2] R. Laxminarayan, A. Duse, C. Wattal, A.K.M. Zaidi, H.F.L. Wertheim, N. Sumpradit, E. Vlieghe, G.L. Hara, I.M. Gould, H. Goossens, C. Greko, A.D. So, M. Bigdeli, G. Tomson, W. Woodhouse, E. Ombaka, A.Q. Peralta, F.N. Qamar, F. Mir, S. Kariuki, Z.A. Bhutta, A. Coates, R. Bergstrom, G.D. Wright, E.D. Brown, O. Cars, Antibiotic resistance—the need for global solutions, Lancet Infect. Dis. 13 (2013) 1057–1098. doi:10.1016/S1473-3099(13)70318-9.

[3] J. O'Neill, Antimicrobial Resistance: Tackling a crisis for the health and wealth of nations, 2014.

[4] E. Tacconelli, E. Carrara, A. Savoldi, S. Harbarth, M. Mendelson, D.L. Monnet, C. Pulcini, G. Kahlmeter, J. Kluytmans, Y. Carmeli, M. Ouellette, K. Outterson, J. Patel, M. Cavaleri, E.M. Cox, C.R. Houchens, M.L. Grayson, P. Hansen, N. Singh, U. Theuretzbacher, N. Magrini, A.O. Aboderin, S.S. Al-Abri, N. Awang Jalil, N. Benzonana, S. Bhattacharya, A.J. Brink, F.R. Burkert, O. Cars, G. Cornaglia, O.J. Dyar, A.W. Friedrich, A.C. Gales, S. Gandra, C.G. Giske, D.A. Goff, H. Goossens, T. Gottlieb, M. Guzman Blanco, W. Hryniewicz, D. Kattula, T. Jinks, S.S. Kanj, L. Kerr, M.-P. Kieny, Y.S. Kim, R.S. Kozlov, J. Labarca, R. Laxminarayan, K. Leder, L. Leibovici, G. Levy-Hara, J. Littman, S. Malhotra-Kumar, V. Manchanda, L. Moja, B. Ndoye, A. Pan, D.L. Paterson, M. Paul, H. Qiu, P. Ramon-Pardo, J. Rodríguez-Baño, M. Sanguinetti, S. Sengupta, M. Sharland, M. Si-Mehand, L.L. Silver, W. Song, M. Steinbakk, J. Thomsen, G.E. Thwaites, J.W. van der Meer, N. Van Kinh, S. Vega, M.V. Villegas, A. Wechsler-Fördös, H.F.L. Wertheim, E. Wesangula, N. Woodford, F.O. Yilmaz, A. Zorzet, Discovery, research, and development of new antibiotics: the WHO priority list of antibiotic-resistant bacteria and tuberculosis, Lancet Infect. Dis. 18 (2018) 318–327. doi:10.1016/S1473-3099(17)30753-3.

[5] S. Rao CV, J. Anné, Bacterial type I signal peptidases as antibiotic targets, Future Microbiol. 6 (2011) 1279–1296. doi:10.2217/fmb.11.109.

[6] S.I. Walsh, Not just an antibiotic target: Exploring the role of type I signal peptidase in bacterial virulence, Bioorg. Med. Chem. 24 (2016) 6370–6378. doi:10.1016/J.BMC.2016.09.048.

[7] A.J. Barrett, N.D. Rawlings, Families and Clans of Serine Peptidases, Arch. Biochem. Biophys. 318 (1995) 247–250. doi:10.1006/abbi.1995.1227.

[8] M. Paetzel, R.E. Dalbey, N.C. Strynadka, The structure and mechanism of bacterial type I signal peptidases: A novel antibiotic target, Pharmacol. Ther. 87 (2000) 27–49. doi:10.1016/S0163-7258(00)00064-4.

[9] J. Schimana, K. Gebhardt, A. Höltzel, D.G. Schmid, R. Süssmuth, J. Müller, R. Pukall, H.-P. Fiedler, Arylomycins A and B, new biaryl-bridged lipopeptide antibiotics produced by Streptomyces sp. Tü 6075. I. Taxonomy, fermentation, isolation and biological activities., J. Antibiot. (Tokyo). 55 (2002) 565–70. doi:10.7164/antibiotics.55.571.

[10] A. Höltzel, D.G. Schmid, G.J. Nicholson, S. Stevanovic, J. Schimana, K. Gebhardt, H.-P. Fiedler, G. Jung, Arylomycins A and B, new biaryl-bridged lipopeptide antibiotics produced by Streptomyces sp. Tü 6075. II. Structure elucidation., J. Antibiot. (Tokyo). 55 (2002) 571–577. doi:10.7164/antibiotics.55.571.

[11] P. Kulanthaivel, A.J. Kreuzman, M.A. Strege, M.D. Belvo, T.A. Smitka, M. Clemens, J.R. Swartling, K.L. Minton, F. Zheng, E.L. Angleton, D. Mullen, L.N. Jungheim, V.J. Klimkowski, T.I. Nicas, R.C. Thompson, S.-B. Peng, Novel lipoglycopeptides as inhibitors of bacterial signal peptidase I., J. Biol. Chem. 279 (2004) 36250–8. doi:10.1074/jbc.M405884200.

[12] A.G. Therien, J.L. Huber, K.E. Wilson, P. Beaulieu, A. Caron, D. Claveau, K. Deschamps, R.G.K. Donald, A.M. Galgoci, M. Gallant, X. Gu, N.J. Kevin, J. Lafleur, P.S. Leavitt, C. Lebeau-Jacob, S.S. Lee, M.M. Lin, A.A. Michels, A.M. Ogawa, R.E. Painter, C.A. Parish, Y.-W. Park, L. Benton-Perdomo, M. Petcu, J.W. Phillips, M.A. Powles, K.I. Skorey, J. Tam, C.M. Tan, K. Young, S. Wong, S.T. Waddell, L. Miesel, Broadening the Spectrum of β-Lactam Antibiotics through Inhibition of Signal Peptidase Type I, Antimicrob. Agents Chemother. 56 (2012) 4662–4670. doi:10.1128/AAC.00726-12.

[13] A.E. Allsop, G. Brooks, G. Bruton, S. Coulton, P.D. Edwards, I.K. Hatton, A.C. Kaura, S.D. McLean, N.D. Pearson, T.C. Smale, R. Southgate, Penem inhibitors of bacterial signal peptidase, Bioorg. Med. Chem. Lett. 5 (1995) 443–448. doi:10.1016/0960-894X(95)00052-U.

[14] A. Allsop, G. Brooks, P.D. Edwards, A.C. Kaura, R. Southgate, Inhibitors of Bacterial Signal Peptidase: A Series of 6-(Substituted oxyethyl)penems., J. Antibiot. (Tokyo). 49

(1996) 921–928. doi:10.7164/antibiotics.49.921.

[15] D.A. Harris, M.E. Powers, F.E. Romesberg, Synthesis and biological evaluation of penem inhibitors of bacterial signal peptidase, Bioorg. Med. Chem. Lett. 19 (2009) 3787–3790. doi:10.1016/J.BMCL.2009.04.034.

[16] C.-H. Yeh, S.I. Walsh, A. Craney, M.G. Tabor, A.-F. Voica, R. Adhikary, S.E. Morris, F.E. Romesberg, Optimization of a β-Lactam Scaffold for Antibacterial Activity via the Inhibition of Bacterial Type I Signal Peptidase., ACS Med. Chem. Lett. 9 (2018) 376–380. doi:10.1021/acsmedchemlett.8b00064.

[17] G. Bruton, A. Huxley, P. O'Hanlon, B. Orlek, D. Eggleston, J. Humphries, S. Readshaw, A. West, S. Ashman, M. Brown, K. Moore, A. Pope, K. O'Dwyer, L. Wang, Lipopeptide substrates for SpsB, the Staphylococcus aureus type I signal peptidase: Design, conformation and conversion to α-ketoamide inhibitors, Eur. J. Med. Chem. 38 (2003) 351–356. doi:10.1016/S0223-5234(03)00040-0.

[18] P. Buzder-Lantos, K. Bockstael, J. Anné, P. Herdewijn, Substrate based peptide aldehyde inhibits bacterial type I signal peptidase, Bioorg. Med. Chem. Lett. 19 (2009) 2880–2883. doi:10.1016/J.BMCL.2009.03.064.

[19] M.D.F.S. Barbosa, S. Lin, J.A. Markwalder, J.A. Mills, J.A. DeVito, C.A. Teleha, V. Garlapati, C. Liu, A. Thompson, G.L. Trainor, M.G. Kurilla, D.L. Pompliano, Regulated expression of the Escherichia coli lepB gene as a tool for cellular testing of antimicrobial compounds that inhibit signal peptidase I in vitro, Antimicrob. Agents Chemother. 46 (2002) 3549–3554. doi:10.1128/AAC.46.11.3549-3554.2002.

[20] J. Ollinger, T. O'Malley, J. Ahn, J. Odingo, T. Parish, Inhibition of the Sole Type I Signal Peptidase of Mycobacterium tuberculosis Is Bactericidal under Replicating and Nonreplicating Conditions, J. Bacteriol. 194 (2012) 2614–2619. doi:10.1128/JB.00224-12.

[21] E.D. Brown, G.D. Wright, Antibacterial drug discovery in the resistance era, Nature. 529 (2016) 336–343. doi:10.1038/nature17042.

[22] F. Giordanetto, J. Kihlberg, Macrocyclic Drugs and Clinical Candidates: What Can Medicinal Chemists Learn from Their Properties?, J. Med. Chem. 57 (2014) 278–295. doi:10.1021/jm400887j.

[23] J. Mallinson, I. Collins, Macrocycles in new drug discovery, Future Med. Chem. 4 (2012) 1409–1438. doi:10.4155/fmc.12.93.

[24] J.L. Hickey, S. Zaretsky, M.A. St. Denis, S. Kumar Chakka, M.M. Morshed, C.C.G. Scully, A.L. Roughton, A.K. Yudin, Passive Membrane Permeability of Macrocycles Can Be Controlled by Exocyclic Amide Bonds, J. Med. Chem. 59 (2016) 5368–5376. doi:10.1021/acs.jmedchem.6b00222.

[25] A.R. Bogdan, N.L. Davies, K. James, Comparison of diffusion coefficients for matched pairs of macrocyclic and linear molecules over a drug-like molecular weight range, Org. Biomol. Chem. 9 (2011) 7727. doi:10.1039/c1ob05996c.

[26] E. Biron, J. Chatterjee, O. Ovadia, D. Langenegger, J. Brueggen, D. Hoyer, H.A. Schmid, R. Jelinek, C. Gilon, A. Hoffman, H. Kessler, Improving Oral Bioavailability of Peptides by Multiple N-Methylation: Somatostatin Analogues, Angew. Chemie Int. Ed. 47 (2008) 2595–2599. doi:10.1002/anie.200705797.

[27] S.A. Kawamoto, A. Coleska, X. Ran, H. Yi, C.-Y. Yang, S. Wang, Design of Triazole-Stapled BCL9 α-Helical Peptides to Target the β-Catenin/B-Cell CLL/lymphoma 9 (BCL9) Protein–Protein Interaction, J. Med. Chem. 55 (2012) 1137–1146. doi:10.1021/jm201125d.

[28] T.L. Aboye, H. Ha, S. Majumder, F. Christ, Z. Debyser, A. Shekhtman, N. Neamati, J.A. Camarero, Design of a Novel Cyclotide-Based CXCR4 Antagonist with Anti-Human Immunodeficiency Virus (HIV)-1 Activity, J. Med. Chem. 55 (2012) 10729–10734. doi:10.1021/jm301468k.

[29] A.C. Rand, S.S.F. Leung, H. Eng, C.J. Rotter, R. Sharma, A.S. Kalgutkar, Y. Zhang, M. V. Varma, K.A. Farley, B. Khunte, C. Limberakis, D.A. Price, S. Liras, A.M. Mathiowetz, M.P. Jacobson, R.S. Lokey, Optimizing PK properties of cyclic peptides: the effect of side chain substitutions on permeability and clearance, Medchemcomm. 3 (2012) 1282. doi:10.1039/c2md20203d.

[30] M.R. Naylor, A.T. Bockus, M.-J. Blanco, R.S. Lokey, Cyclic peptide natural products chart the frontier of oral bioavailability in the pursuit of undruggable targets, Curr. Opin. Chem. Biol. 38 (2017) 141–147. doi:10.1016/J.CBPA.2017.04.012.

[31] M. De Rosa, L. Lu, E. Zamaratski, N. Szałaj, S. Cao, H. Wadensten, L. Lenhammar, J. Gising, A.K. Roos, D.L. Huseby, R. Larsson, P.E. Andrén, D. Hughes, P. Brandt, S.L.

Mowbray, A. Karlén, Design, synthesis and in vitro biological evaluation of oligopeptides targeting E. coli type I signal peptidase (LepB), Bioorganic Med. Chem. 25 (2017) 897–911. doi:10.1016/j.bmc.2016.12.003.

[32] P.A. Smith, R.I. Roberts, Tucker Curran, Higuchi, P. Paraselli, M.F.T. Koehler, J.J. Crawford, WO2015023898, 2015.

[33] R.I. Higuchi, T.C. Roberts, P.A. Smith, D. Campbell, P. Paraselli, WO2013123456, 2013.

[34] J.T. Bien, M.J. Eschner, B.D. Smith, Molecular recognition with boron acids. Part 10. A neutral paraquat receptor that uses oriented dipoles produced by dative B-N bonds, J. Org. Chem. 60 (1995) 4525–4529. doi:10.1021/jo00119a033.

[35] A. Ahmad Fuaad, F. Azmi, M. Skwarczynski, I. Toth, Peptide Conjugation via CuAAC "Click" Chemistry, Molecules. 18 (2013) 13148–13174. doi:10.3390/molecules181113148.

[36] C. Luo, P. Roussel, J. Dreier, M.G.P. Page, M. Paetzel, Crystallographic analysis of bacterial signal peptidase in ternary complex with arylomycin A2 and a beta-sultam inhibitor., Biochemistry. 48 (2009) 8976–84. doi:10.1021/bi9009538.

[37] M. Paetzel, Structure and mechanism of Escherichia coli type I signal peptidase., Biochim. Biophys. Acta. 1843 (2014) 1497–1508. doi:10.1016/j.bbamcr.2013.12.003.

[38] P.Y.S. Lam, C.G. Clark, S. Saubern, J. Adam, K.M. Averill, D.M.T. Chan, A. Combs, Copper Promoted Aryl/Saturated Heterocyclic C-N Bond Cross-Coupling with Arylboronic Acid and Arylstannane, Synlett. (2000) 674–676. doi:10.1055/s-2000-6628.

[39] Y. Xu, J. Zhao, H. Chen, W. Wu, H. Jiang, A convenient regioselective synthesis of cyclopentadienones via palladium-catalyzed [2+2+1] cyclocarbonylation of alkynes., Chem. Commun. (Camb). 50 (2014) 2488–90. doi:10.1039/c3cc48308h.

[40] Y.J. Kim, P. Wang, M. Navarro-Villalobos, B.D. Ronde, J.M. Derryberry, D.Y. Gin, Synthetic studies of complex immunostimulants from Quillaja saponaria: Synthesis of the potent clinical immunoadjuvant QS-21Aapi, J. Am. Chem. Soc. 128 (2006) 11906–11915. doi:10.1021/ja062364i.

[41] F. Himo, T. Lovell, R. Hilgraf, V. V. Rostovtsev, L. Noodleman, K.B. Sharpless, V. V.

Fokin, Copper(I)-Catalyzed Synthesis of Azoles. DFT Study Predicts Unprecedented Reactivity and Intermediates, J. Am. Chem. Soc. 127 (2005) 210–216. doi:10.1021/ja0471525.

[42] N. Sewald, H.-D. Jakubke, Peptides: Chemistry and Biology, Wiley-VCH Verlag GmbH & Co. KGaA, Weinheim, FRG, 2003. doi:10.1002/352760068X.ch1.

[43] M. Bodanszky, Peptide chemistry : a practical textbook, Springer-Verlag, Berlin, Heidelberg, 1988.

[44] A.K. Ghosh, S. Gemma, J. Takayama, A. Baldridge, S. Leshchenko-Yashchuk, H.B. Miller, Y.-F. Wang, A.Y. Kovalevsky, Y. Koh, I.T. Weber, H. Mitsuya, Potent HIV-1 protease inhibitors incorporating meso-bicyclic urethanes as P2-ligands: structure-based design, synthesis, biological evaluation and protein-ligand X-ray studies., Org. Biomol. Chem. 6 (2008) 3703–13. doi:10.1039/b809178a.

[45] V. VanRheenen, R.C. Kelly, D.Y. Cha, An improved catalytic OsO4 oxidation of olefins to *cis*-1,2-glycols using tertiary amine oxides as the oxidant, Tetrahedron Lett. 17 (1976) 1973–1976. doi:10.1016/S0040-4039(00)78093-2.

[46] O. Mitsunobu, M. Yamada, Preparation of Esters of Carboxylic and Phosphoric Acid *via* Quaternary Phosphonium Salts, Bull. Chem. Soc. Jpn. 40 (1967) 2380–2382. doi:10.1246/bcsj.40.2380.

[47] H.R. Snyder, J.A. Kuck, R.J. Johnson, Organoboron Compounds, and the Study of Reaction mechanisms. Primary Aliphatic Boronic Acids, J. Am. Chem. Soc. 60 (1938) 105–111. doi:10.1021/ja01268a033.

[48] E. Lindhagen, P. Nygren, R. Larsson, The fluorometric microculture cytotoxicity assay, Nat. Protoc. 3 (2008) 1364–1369. doi:10.1038/nprot.2008.114.

[49] I. Sosič, M. Anderluh, M. Sova, M. Gobec, I. Mlinarič Raščan, A. Derouaux, A. Amoroso, M. Terrak, E. Breukink, S. Gobec, Structure–Activity Relationships of Novel Tryptamine-Based Inhibitors of Bacterial Transglycosylase, J. Med. Chem. 58 (2015) 9712–9721. doi:10.1021/acs.jmedchem.5b01482.

[50] L.H. Kondejewski, M. Jelokhani-Niaraki, S.W. Farmer, B. Lix, C.M. Kay, B.D. Sykes, R.E.W. Hancock, R.S. Hodges, Dissociation of antimicrobial and hemolytic activities in cyclic peptide diastereomers by systematic alterations in amphipathicity, J. Biol.

Chem. 274 (1999) 13181–13192. doi:10.1074/jbc.274.19.13181.

[51] T. V. Magee, M.F. Brown, J.T. Starr, D.C. Ackley, J.A. Abramite, J. Aubrecht, A. Butler, J.L. Crandon, F. Dib-Hajj, M.E. Flanagan, K. Granskog, J.R. Hardink, M.D. Huband, R. Irvine, M. Kuhn, K.L. Leach, B. Li, J. Lin, D.R. Luke, S.H. MacVane, A.A. Miller, S. McCurdy, J.M. McKim, D.P. Nicolau, T.-T. Nguyen, M.C. Noe, J.P. O'Donnell, S.B. Seibel, Y. Shen, A.F. Stepan, A.P. Tomaras, P.C. Wilga, L. Zhang, J. Xu, J.M. Chen, Discovery of Dap-3 Polymyxin Analogues for the Treatment of Multidrug-Resistant Gram-Negative Nosocomial Infections, J. Med. Chem. 56 (2013) 5079–5093. doi:10.1021/jm400416u.

[52] M. Erdélyi, V. Langer, A. Karlén, A. Gogoll, Insight into β-hairpin stability: a structural and thermodynamic study of diastereomeric β-hairpin mimetics, New J. Chem. 26 (2002) 834–843. doi:10.1039/b111241d.

[53] D. Ranganathan, V. Haridas, S. Kurur, R. Nagaraj, E. Bikshapathy, A.C. Kunwar, A.V.S. Sarma, M. Vairamani, Norbornene-Constrained Cyclic Peptides with Hairpin Architecture: Design, Synthesis, Conformation, and Membrane Ion Transport, J. Org. Chem. 65 (2000) 365–374. doi:10.1021/jo9912045.

[54] E. Harder, W. Damm, J. Maple, C. Wu, M. Reboul, J.Y. Xiang, L. Wang, D. Lupyan, M.K. Dahlgren, J.L. Knight, J.W. Kaus, D.S. Cerutti, G. Krilov, W.L. Jorgensen, R. Abel, R.A. Friesner, OPLS3: A Force Field Providing Broad Coverage of Drug-like Small Molecules and Proteins., J. Chem. Theory Comput. 12 (2016) 281–296. doi:10.1021/acs.jctc.5b00864.

[55] H.M. Berman, J. Westbrook, Z. Feng, G. Gilliland, T.N. Bhat, H. Weissig, I.N. Shindyalov, P.E. Bourne, The Protein Data Bank., Nucleic Acids Res. 28 (2000) 235–242. doi:10.1093/nar/28.1.235.

[56] Schrödinger Release 2017-1: Schrödinger Suite 2017-1 Protein Preparation Wizard; Epik, Schrödinger, LLC, New York, NY, 2016; Impact, Schrödinger, LLC, New York, NY, 2016; Prime, Schrödinger, LLC, New York, NY, 2017.

[57] Schrödinger Release 2017-1: Maestro, Schrödinger, LLC, New York, NY, 2017.